



# The University of Bradford Institutional Repository

<http://bradscholars.brad.ac.uk>

This work is made available online in accordance with publisher policies. Please refer to the repository record for this item and our Policy Document available from the repository home page for further information.

To see the final version of this work please visit the publisher's website. Available access to the published online version may require a subscription.

**Link to Publisher's version:** <https://doi.org/10.1166/jbt.2014.1224>

**Citation:** Bye FJ, Bullock AJ, Singh R, Sefat F, Roman S and MacNeil S (2014) Development of a basement membrane substitute incorporated into an electrospun scaffold for 3D skin tissue engineering. *Journal of Biomaterials and Tissue Engineering*. 4: 1-7.

**Copyright statement:** © 2014 American Scientific Publishers. Reproduced with the permission of the publisher.



# Development of a Basement Membrane Substitute Incorporated Into an Electrospun Scaffold for 3D Skin Tissue Engineering

Frazer J. Bye<sup>1</sup>, Anthony J. Bullock<sup>1</sup>, Rita Singh<sup>2</sup>,  
Farshid Sefat<sup>1</sup>, Sabiniano Roman<sup>1</sup>, and Sheila MacNeil<sup>1,\*</sup>

<sup>1</sup>Materials Science and Engineering, Kroto Research Institute, University of Sheffield, Sheffield S3 7HQ, United Kingdom

<sup>2</sup>Defence Laboratory, Defence Research and Development Organization, Jodhpur 342011, India

A major challenge in the production of 3D tissue engineered skin is the recreation of the basement membrane region to promote secure attachment and yet segregation of keratinocytes from the dermal substitute impregnated with fibroblasts. We have previously shown that simple electrospun scaffolds provide fibres on which the cells attach, proliferate, and self-sort into epithelium and dermis. In a development of this in this study tri-layered scaffolds were then electrospun from poly L-lactic acid and poly hydroxybutyrate-co-hydroxyvalerate. In these a central layer of the scaffolds comprising nano-porous/nano-fibrous poly hydroxybutyrate-co-hydroxyvalerate fibres was interwoven into the bulk micro-porous poly L-lactic acid microfibers to mimic the basement membrane. Keratinocytes and fibroblasts seeded onto these scaffolds and cultured for 2 weeks showed that neither cell type was able to cross the central nano-porous barrier (shown by SEM, and fluorescence monitoring with CellTracker™) while the micro-fibrous poly L-lactic acid provided a scaffold on which keratinocytes could create an epithelium and fibroblasts could create a dermal substitute depositing collagen. Although cells did not penetrate this barrier the interaction of cells was still evident-essential for epithelial development.

## Keywords:

## 1. INTRODUCTION

There has been an increasing interest in the tissue engineering of skins using natural or synthetic matrices for treatment of burns and other skin injuries to restore barrier function or to initiate wound healing.<sup>1</sup> Such a tissue engineering approach can potentially remove the fundamental limitation of skin repair-the lack of sufficient suitable donor material. Tissue-engineered skin is created by harvesting and expanding appropriate skin cells, seeding them into a three-dimensional scaffold and inducing them to proliferate, differentiate and develop into a tissue for implantation. Skin comprises several different cell types which reside on and in the dermis respectively. Keratinocytes are the most common cell type in the epidermis, forming a proliferative layer of dividing cells attached to the basement membrane of the papillary dermis. Supra-basal keratinocytes stratify and differentiate to form the surface cornified lipid rich barrier layer. Fibroblasts reside within the collagen/fibrin matrix of the dermis

and are crucial in both matrix repair and renewal, but the cytokine interplay between fibroblasts and keratinocytes is required for the successful creation of a functional normal epidermis.<sup>2</sup> The dermal matrix which supports the epidermis provides mechanical support, strength, flexibility and elasticity for the skin. Its upper papillary surface provides basement membrane allowing strong attachment and promotion of proliferation for keratinocytes.<sup>3,4</sup> Its matrix provides the ECM carrying capillaries supplying nutrition to the epithelium and waste removal and immune surveillance in addition to sweat glands and anchorage for hair follicles. The basement membrane is a dense, highly cross-linked sheet of extracellular matrix that structurally underlies all epithelia, it is selectively permeable to the cells of the skin-segregating keratinocytes and fibroblasts at the dermal/epidermal junction.<sup>5-7</sup> In 2D and 3D culture systems where rapid keratinocyte growth is promoted, keratinocytes not only inhibit fibroblast proliferation, but can detach fibroblasts from the surface on which they are growing-removing them despite their contribution to keratinocyte growth and development.

\*Author to whom correspondence should be addressed.

The dermis is anything but a simple scaffold, and the development of a scaffold to replace it—even during short term wound healing requires a scaffold to perform at least some of the basic functions of dermis. Scaffolds should be biocompatible and exhibit mechanical properties similar to those of target tissue. Moreover, the scaffold should have structural and properties mimicking those of the dermis supporting cell behaviour such as adhesion, migration, proliferation, and differentiation.<sup>8</sup>

Artificial basement membrane regions in tissue engineered models are not common due to the complex nature of the proteins involved, though the use of the animal tumour derived matrix extract known as matrigel can provide some of the functionality of a BM.<sup>9–11</sup> Where keratinocytes and fibroblasts are cultured separately on an appropriate matrix such as a collagen/fibrin gel they can recreate a functional basement membrane though this takes a significant time, and is mechanically weak compared to skin.<sup>12</sup>

Electrospinning is a popular and versatile method for producing scaffolds for 3D tissue engineering and regenerative medicine, and it can give 3D open porous structures which approximate to the structure of the dermis.<sup>13–16</sup> The use of synthetic scaffolds avoids the potential disease transmission associated with native tissues such as bovine collagen but in common with other synthetic scaffolds a monolith of fibres gives no barrier or partition of the epidermal and stromal cells.<sup>17</sup> Bye et al. created bi- and tri-layer scaffolds of micro-porous poly L-lactic acid (PLLA) electrospun onto nano-porous poly hydroxybutyrate-co-hydroxyvalerate (PHBV) scaffolds-creating a cell impermeable sheet coated on one or both sides with a micro-porous scaffold capable of segregating cells and supporting growth. In these early experiments delamination of the nano-porous layer from the micro-porous layer was a potential issue.<sup>18</sup> We have further developed this scaffold so that the nano-porous layer can be interwoven within a PLLA micro-porous scaffold. The PHBV and PLLA fibres co-mingle as a central cell impermeable layer to provide segregation and to prevent delamination.

In this study the potential of the nano-fibrous PHBV membrane of the tri-layered scaffold to act as a surrogate basement membrane was investigated by seeding these tri-layered scaffolds with human epithelial keratinocytes and dermal fibroblasts and assessing the maintenance of segregation. Such a tissue construct may be of use as both a research model and as a tissue engineered replacement for split-thickness skin when constructed with the patient's own laboratory expanded skin cells.

## 2. METHODS

### 2.1. Preparation of Electrospun Scaffolds

Micro-fibrous PLLA and nano-fibrous PHBV scaffolds were electrospun using parameters as described by Bye et al.<sup>19</sup> PLLA (10 wt% solution in Dichloromethane

(DCM) and PHBV (10 wt% solution in 90 wt% DCM/10 wt% methanol) was pumped from 4 syringes at  $40 \mu\text{L min}^{-1}$  per syringe. For PLLA a needle to collector distance of 17 cm was used while for PHBV, a distance of 10 cm was used. The syringe needles were charged to +17 kV (73030 P, Genvolt, Shropshire, UK) and polymer solutions spun onto an earthed rotating (400 RPM) aluminium foil coated mandrel (20 cm wide, 10 cm diameter) (Fig. 1(A)). PLLA and PHBV were setup in separate syringe pumps on either side of the rotating mandrel and charged by individual power supplies. Tri-layers were spun by sequentially spinning first 8 ml PLLA, 4 ml of PHBV was simultaneously spun with 4 ml PLLA from a matching spinning setup on the other side of the mandrel then 8 ml PLLA was spun alone, creating a PLLA-PHBV/PLLA-PLLA tri-layer construct. A PLLA monolayer scaffold was electrospun by repeating this method but omitting the spinning of PHBV.

### 2.2. Tissue Engineered Skin Culture on PLLA/PHBV Scaffolds

Human keratinocytes and fibroblasts were obtained from split thickness skin grafts taken from skin obtained from elective breast reductions or abdominoplasties with fully informed consent and stored under HTA Tissue Bank license no 12179.

Skin was cut into  $5 \times 5$  mm pieces and digested in trypsin solution ( $1 \text{ mg} \cdot \text{mL}^{-1}$  porcine trypsin, 0.1% w/v D-glucose in PBS) for 18 hours at  $4^\circ\text{C}$ . Keratinocytes were then gently scraped from the dermal-epidermal junction region into Green's medium (Dulbecco's modified Eagle's medium (DMEM) and Ham's F12 medium in a 3:1 (v/v) ratio supplemented with 10% (v/v) fetal calf serum (FCS),  $0.1 \mu\text{M}$  cholera toxin, 10 ng/ml epidermal growth factor (EGF),  $0.4 \mu\text{g/ml}$  hydrocortisone, 0.18 mM adenine,  $5 \mu\text{g/ml}$  insulin, 2 mM glutamine,  $0.2 \mu\text{M}$  triiodothyronine,  $0.625 \mu\text{g/ml}$  amphotericin B, 100 IU/ml penicillin and  $100 \mu\text{g/ml}$  streptomycin) after. Keratinocytes were co-cultured with an i3T3 feeder layer prior to use and passage 1–2 keratinocytes were used in experiments.

Fibroblasts were isolated from de-epithelialised dermis by collagenase digestion (0.1% collagenase in DMEM) overnight at  $37^\circ\text{C}$ . After pelleting the cells at 400 g for 10 mins, fibroblasts were cultured in DMEM (supplemented with 10% v/v FCS and  $0.625 \mu\text{g/ml}$  amphotericin B, 100 IU/ml penicillin and  $100 \mu\text{g/ml}$  streptomycin and 2 mM glutamine), and passage 4–9 fibroblasts were used in experiments.

Tri-layer (PLLA-PHBV/PLLA-PLLA) and monolayer (PLLA) electrospun scaffolds ( $2 \text{ cm} \times 2 \text{ cm}$ ) were sterilised (70% v/v ethanol in  $\text{dH}_2\text{O}$ ) for 10 mins, washed with PBS, and placed in 6-well plates. A 1 cm diameter culture well was formed on the scaffold using a 1 cm diameter stainless steel ring and  $1 \times 10^5$  fibroblasts (in DMEM supplemented with 10% FCS v/v) seeded inside. Constructs were cultured for 2 days at  $37^\circ\text{C}$  and 5%  $\text{CO}_2$ . Scaffolds were

them turned over and  $3 \times 10^5$  keratinocytes were seeded onto each scaffold in Green's medium. After a further 2 days of culture the constructs were raised to an air-liquid interface on stainless steel grids and cultured for a further 7 and 14 days.

### 2.3. Scanning Electron Microscopy (SEM) of Scaffolds

Constructs were removed from culture medium, washed briefly with PBS then fixed in 2.5% glutaraldehyde for 10 minutes. The specimens were then incubated with 2 ml of 0.1 M sodium cacodylate buffer for 3–5 minutes then in 2 ml of 2.5% glutaraldehyde for 30 mins. Each sample was then rinsed with sodium cacodylate buffer to remove any remaining glutaraldehyde. Secondary fixation was carried out in 2% osmium tetroxide (aqueous) for 2 hours before incubation in 2 ml of 0.1 M sodium cacodylate buffer for 15 min. Samples were then dehydrated in ascending grades of alcohol then dried overnight, bisected and mounted on 12.5 mm stubs. Samples were then sputter coated with gold (25 nm thick approximately) then examined using a scanning electron microscope (FEI XL-20 SEM, Philips, Guildford, UK) at an accelerating voltage of 20 kV.

### 2.4. Assessment of Viability of Tissue Engineered Skin

Viable cell density of tissue engineered skin was assessed using the MTT (3-(4,5-dimethylthiazol-2-yl)-2,5-diphenyl tetrazolium bromide) Eluted Stain Assay (MTT-ESTA). Intracellular dehydrogenase activity reduces MTT to a purple coloured formazan salt. In healthy viable cells, MTT is reduced to a purple coloured formazan salt by the activity of the mitochondrial enzyme succinyl dehydrogenase. Electrospun scaffolds with the cells cultured for 7 and 14 days were washed three times in PBS and then incubated with MTT solution (0.5 mg/ml MTT in PBS, 2 ml per well of 6-well plate) for 45 min at 37 °C and in a 95% air/5% CO<sub>2</sub> environment. After 45 min samples were washed with PBS, and the samples incubated in 100 µl Cellusolve™ for 10 min. The optical density at 540 nm (with a reference at 630 nm) was then measured using a spectrophotometer (Bio-TEK, NorthStar Scientific LTD, Leeds, UK).

### 2.5. Quantification of Collagen Deposition in Scaffolds

Collagen deposition on scaffold fibres was measured by using a Sirius red stain. Constructs were washed three times in PBS then fixed in 3.7% formaldehyde in PBS for 10 minutes. After washing in PBS 1 ml of 0.1% w/v Direct Red 80 (Sigma-Aldrich) in saturated picric acid was added and samples incubated for 18 hours at room temperature. Constructs were rinsed with water until no further colour was eluted. Samples were then dried overnight before bound stain was eluted with 500 µl 1:1 v/v 0.2 M NaOH in methanol 1:1 for 15 min. Optical density at 490 nm was then measured using a spectrophotometer (Bio-TEK, NorthStar Scientific LTD, Leeds, UK).

### 2.6. Immunostaining for Keratin to Identify Keratinocytes

Immunostaining of keratins using pancytokeratin antibody (ABD Serotec LTD, UK) was used to identify keratinocytes in this study. Scaffolds cultured with cells were fixed in 3.7% formaldehyde in PBS for 10 minutes and washed 3 times with PBS. Samples were then permeabilized with 0.5% w/v Triton X100 in PBS for 20 minutes at room temperature. After blocking for 1 hour with 1% w/v bovine serum albumin (BSA) in PBS, cells were incubated at 40 °C overnight with primary antibody (mouse anti-cytokeratin, diluted 1:50 in 1% w/v BSA in PBS). Samples were then washed with PBS and incubated with biotinylated anti-mouse secondary antibody (1:1000 in PBS) for 1.5 hours at room temperature. After washing with PBS samples were incubated for one hour with Texas Red streptavidin (1:100 in PBS (Life Technologies, USA)) and DAPI (4',6-diamidino-2-phenylindole, 1 µg/ml in PBS (Life Technologies, USA)). After further washing with PBS (three times) fluorescence emission was visualized with Axon ImageXpress (Axon instruments, USA) fluorescence microscope. Micrographs were captured at  $\lambda_{\text{ex}} - 570 \text{ nm}/\lambda_{\text{em}} - 620 \text{ nm}$  (pancytokeratin) and  $\lambda_{\text{ex}} - 365 \text{ nm}/\lambda_{\text{em}} - 460 \text{ nm}$  (DAPI).

### 2.7. Cell Tracker Labelling of Keratinocytes and Fibroblasts

Prior to seeding cells on scaffolds, CellTracker™ Green and CellTracker™ Red (Invitrogen Ltd, USA) were used to label keratinocytes and fibroblasts respectively. Adherent cells in culture flasks were rinsed with serum free culture media before CellTracker™ Red or Green (50 µg in 5 ml of serum-free culture medium) was added to culture flasks and incubated at 37 °C for 45 minutes. After washing with Greens medium, cells were incubated in Greens medium for a further 30 minutes at 37 °C. Cells were then seeding onto scaffolds as previously described. Labelled cells were imaged in an Axon ImageExpress Microscope (Molecular Devices, Sunnyvale, USA) at  $\lambda_{\text{ex}} - 570 \text{ nm}/\lambda_{\text{em}} - 620 \text{ nm}$  (Cell Tracker Red) and  $\lambda_{\text{ex}} - 480 \text{ nm}/\lambda_{\text{em}} - 533 \text{ nm}$  (Cell Tracker Green).

### 2.8. Statistics

Statistical significance was calculated using Students paired *T*-test, and *p* values of < 0.05 were considered statistically significant.

## 3. RESULTS

Tri-layered (PLLA-PHBV/PLLA-PLLA) and mono-layered (PLLA) scaffolds were fabricated by electrospinning (Fig. 1(B)), SEM photographs of sections through each scaffold show the tri-layer scaffold to have a region of intermingling of the micro- and nano-fibres in a discrete layer approximately 20 µm thick (Figs. 2(A)

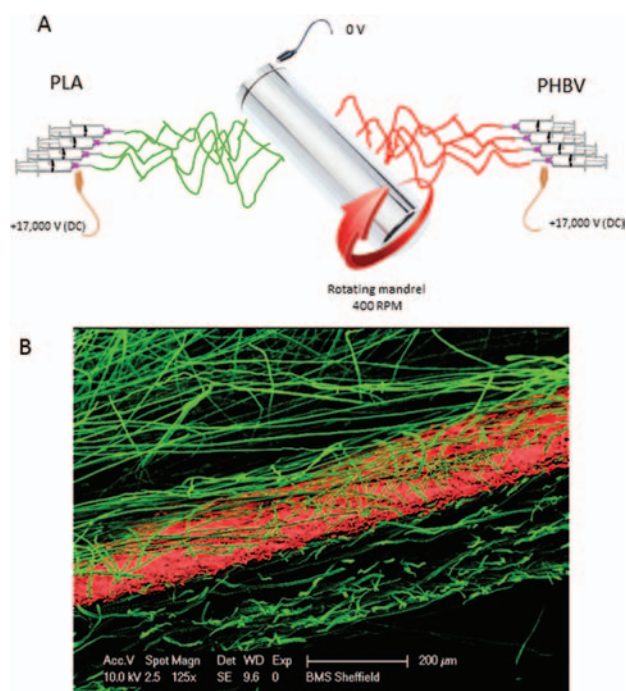


**Fig. 1.** (A) Diagram of the dual polymer electrospinning rig used to create tri-layered membrane. Microfibres (green) are electrospun on one side of the mandrel while PHBV nanofibres (red) are spun at the same time on the opposite side of the rotating mandrel. (B) SEM image of the arrangement of micro (green) and nano (red) fibres in trilayer scaffold. Scale bar represents 200  $\mu\text{m}$ .

and (B)) which is missing from the monolayer scaffold (Figs. 2(C) and (D)). The central region of nano-fibres ( $519 \pm 50.65$  nm diameter) entangled with microfibres ( $2.36 \pm 0.15$   $\mu\text{m}$  diameter) forms a continuous layer region which appears to be almost nano-porous (pores are  $1.37 \pm 0.097$   $\mu\text{m}$  whereas the remaining bulk of the scaffold has pores of  $13.29 \pm 2.24$   $\mu\text{m}$ ). Monolayer PLLA scaffolds had uniformly randomly arranged fibres ( $3.70 \pm 0.29$   $\mu\text{m}$  diameter) with pores of  $19.39 \pm 1.49$   $\mu\text{m}$  and these parameters were not significantly different to those of the microfibres of the tri-layer scaffold.

Keratinocytes and fibroblasts seeded on the upper and lower surfaces respectively of mono- and tri-layer scaffolds surface proliferated over time as shown by MTT staining of 7 and 14 day cultures and there were no significant differences between cell growth on the tri- and mono layer scaffolds (Fig. 3). SEM images show the cells attached to both scaffolds, keratinocytes forming an epithelial sheet covering the upper surface of the scaffolds by 14 days (Fig. 4). The lower surfaces of both tri and mono layer scaffolds showed the presence of fibroblasts and the suggestion of matrix proteins on the scaffold fibres.

This pattern of apparent cell segregation was also seen in H&E sections where keratinocytes were seen to extend from the upper surface of the scaffold down to the interwoven barrier and no further, and the lower portion has some but few fibroblasts (Fig. 5(A)). Sections of monolayer

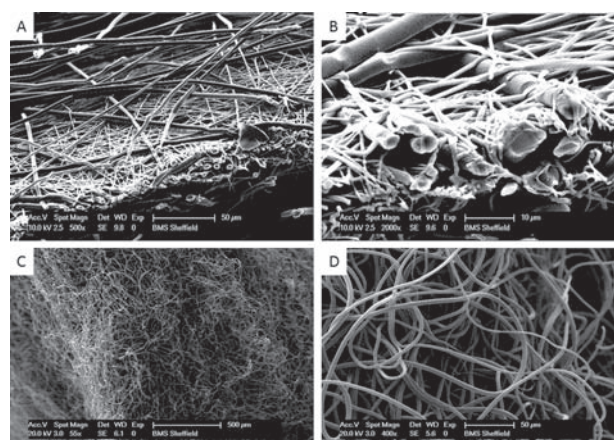


**Fig. 2.** SEM of sections through tri-layer and monolayer scaffolds. (A) and (B) show the micro/nano fibres in the central barrier region of the scaffold. (C) and (D) detail the monolayer scaffold composed of PLLA microfibres. Scale bars as shown in each individual photograph.

scaffolds showed no such organization suggesting that cells were unable to cross this central barrier region of the tri-layer scaffolds but were free to colonise the entire thickness of the monolayer scaffolds (Fig. 5(B)). (Please note that paraffin fixing and dewaxing using solvents dissolves most of the scaffolds hence imaging results by this method is challenging compared to SEM and immunostaining).

To further verify segregation of cells, cell tracker loaded cells were added to scaffolds on opposing sides of the interwoven barrier, and their ability to cross the thickness of each scaffold assessed. Figure 6 shows cell tracker labelled cells were found to be segregated by the interwoven barrier of the tri-layer scaffold as keratinocytes (labelled with green CellTracker™) were only found on the upper surface of tri-layer scaffolds while in monolayer scaffolds they could also be seen on the lower surface. Similarly fibroblasts (labelled with green cell tracker) could only be found in the lower region of tri-layer scaffolds but were seen throughout the monolayer scaffold.

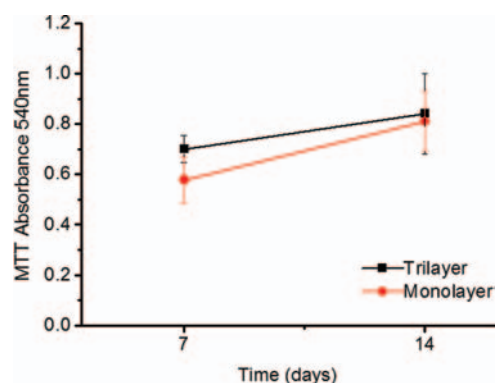


**Fig. 3.** Viability of keratinocytes and fibroblasts cultured on tri-layer and monolayer scaffold for 7 and 14 days. Results shown represent mean  $\pm$  SD ( $n = 6$ ).

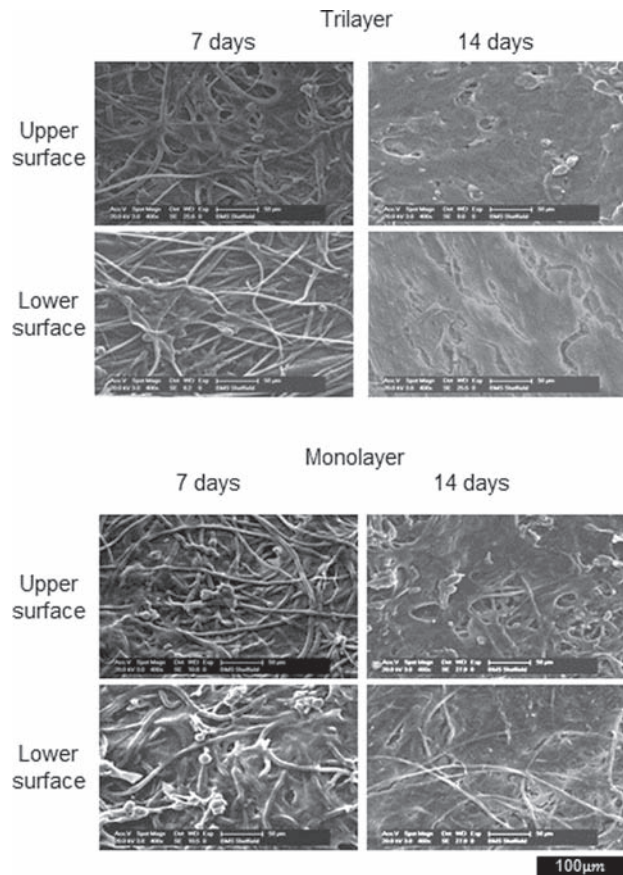


**Fig. 4.** SEM images of keratinocytes and fibroblasts cultured on tri-layer and monolayer scaffold for 7 and 14 days, upper and lower surfaces of tri-layer and monolayer scaffolds. Scale bars = 100 μm.

Positive identification of keratinocytes was made by immunostaining of the keratinocytes for keratin production and this confirmed their location in the upper part of the tri-layer and throughout the monolayer scaffolds. An image showing expression of pancytokeratin on the scaffold seeded with keratinocytes is presented in Figure 7. Cells positive for pan-cytokeratin were not seen in the lower layers of tri-layer scaffolds—only the DAPI stained nuclei of pancytokeratin negative cells (fibroblasts) were seen. Again, as before, such segregation was not seen in monolayer scaffolds. Total collagen production by cells on the scaffolds increased over time on each scaffold, as

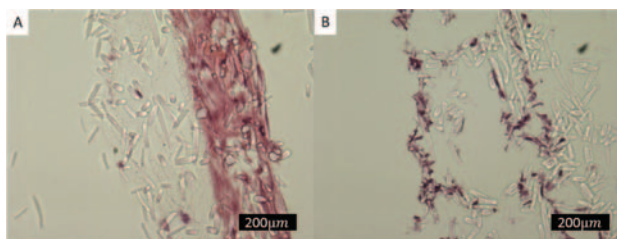


**Fig. 5.** H&E sections of (A) PLLA-PHBV/PLLA-PLLA tri-layer and (B) PLLA monolayer seeded with keratinocytes and fibroblasts after 14 days of culture. 100x magnification, scale bar = 200 μm.

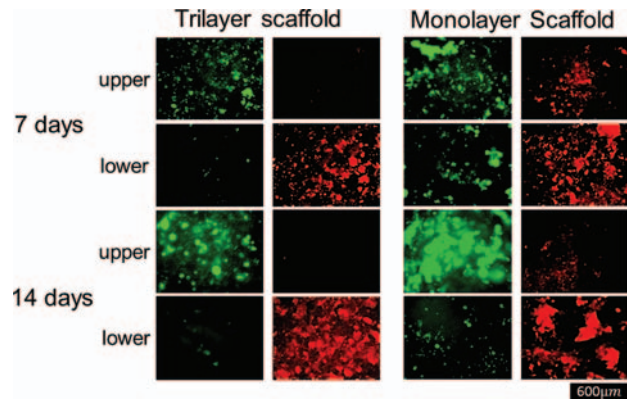


**Fig. 6.** Celltracker™ labelled keratinocytes (green) and fibroblasts (red) cultured on tri-layer and monolayer scaffolds for 7 and 14 days. 100x magnification scale bar = 600 μm.

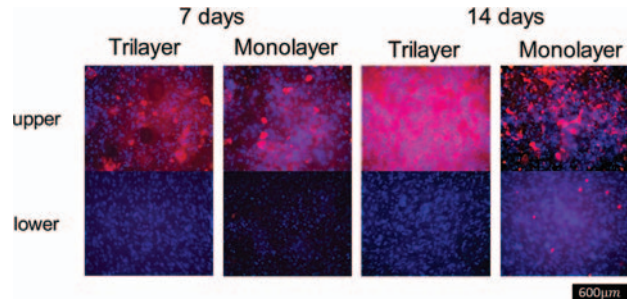


**Fig. 7.** Pancytokeratin expression (red) by keratinocytes cultured on tri-layer and monolayer scaffolds for 7 and 14 days, all cells were counterstained with DAPI (blue). 100x magnification, scale bar = 600 μm.

seen by the intense red staining seen in all cell seeded scaffolds. However there was significantly more collagen found on the tri-layer scaffolds compared to the monolayer scaffolds at both 7 and 14 days of culture ( $P < 0.05$ , Fig. 8).

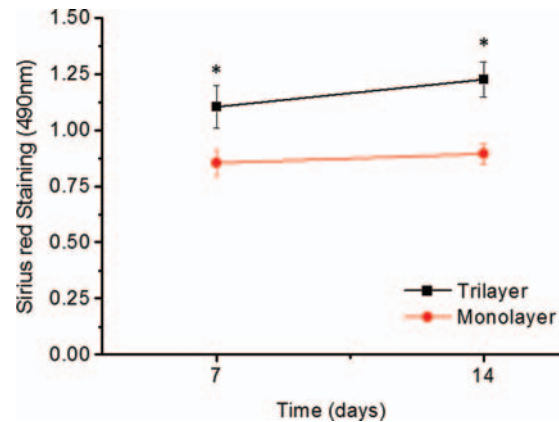


**Fig. 8.** Collagen deposition measured using Sirius red staining of co-cultures of keratinocytes and fibroblasts on tri-layer scaffolds and monolayer scaffolds after 7 and 14 days. Results shown represent mean ± SD ( $n = 6$ ).

#### 4. DISCUSSION

Our aim was to produce a biodegradable scaffold containing a basement membrane substitute that would simplify the production of 3D tissue engineered skin for clinical use.

In this study we have shown that a simple barrier can be made within an electrospun scaffold to recreate the cell segregation/barrier function of the basement membrane of the human dermis.

This allowed the culture of keratinocytes and fibroblasts in conditions where they could have communication via cytokine signalling but remain as separate populations of cells. Synthetic polymer scaffolds are increasingly common in tissue engineering, providing a surface for cell growth and a mechanical support structure for the developing tissue. However biological scaffolds such as de-epidermised dermis (DED) or amnion provide more than a simple scaffold, they possess attachment proteins which provide location and behavioural cues for the cells growing on them - the basement membrane.

One function of the basement membrane is to provide segregation for cells to prevent one cell type over growing the other—but still allowing cytokine crosstalk—which is critical in the creation of a fully stratified functional epidermis. This could be partially provided by selectively coating the scaffold with matrigel—however this would preclude the clinical use of such scaffolds due to the animal cancer cell line origin (a hamster fibrosarcoma) of the BM proteins in matrigel.<sup>20, 21</sup>

The current study focuses on the fabrication of a tri-layered electrospun scaffold using poly lactic acid/poly hydroxybutyrate-co-hydroxyvalerate/poly(lactic acid) (PLLA-PHBV/PLLA-PLLA) exploring the potential of an interwoven nano-fibrous PHBV/PLLA layer to act as a basement membrane substitute for the organization of epidermal and dermal cells for 3D skin construction.

The potential of the tri-layered electrospun scaffolds for 3D skin construction was evaluated by observing their ability to support both the adhesion and proliferation of keratinocytes and fibroblasts after culturing on their surfaces for 7 and 14 days. Scanning electron microscopy images demonstrated adhesion and proliferation of epidermal and dermal cells on the tri-layered and mono-layered scaffold and the surface coverage after 7 days and 14 days on the tri-layered scaffold was the same as that on the control mono-layered PLLA scaffolds.

Images of the cross-section of the tri-layered scaffold show that the PHBV nano-fibrous layer of the tri-layered scaffold may mimic the basement membrane, the nano-fibrous layer of the tri-layered scaffold obstructed the cellular migration of keratinocytes and fibroblasts from the two opposite PLLA scaffold layers. While the viability of cells on the scaffolds was not affected by the presence of the nano-porous PHBV layer, there was a small but significant increase in collagen deposition on the tri-layered scaffold. This deposition would be the start of

the skin cells remodelling the scaffold from a synthetic scaffold to a collagenous tissue. It is known that when keratinocytes and fibroblasts are co-cultured they begin to produce basement membrane proteins.<sup>22</sup> However in our experience based on looking at the formation of hemidesmosomes in reconstructed skin based on decellularised dermis they failed to achieve any structural organization even after 3 weeks *in vitro* unless there was some basement membrane already present in which case they were able to form hemidesmosomes which help anchor the keratinocytes to the underlying dermal collagen.<sup>23</sup> In the current study we have provided cells with a physically dense nano-fibrous mesh as a basement membrane substitute. Alternative approaches of introducing natural ECM proteins may well work but are rarely going to be suitable for scale - up for clinical use for reasons of cost and more importantly regulatory concerns about safety will mean that such ECM proteins must be sourced so they are no risk to the patient-implicating recombinant proteins or synthesised peptide sequences from these proteins. Our approach is simpler and cheaper and poses no clinical risks.

In scaffolds where there is no barrier to growth of keratinocytes, epithelial growth may ultimately fill up the entire scaffold usurping the fibroblasts—as seen in HACAT seeded mono- but not tri-layer scaffolds (data not shown). The cell impermeable barrier creates a niche or refuge for fibroblasts preventing displacement and ensuring their continued presence. This preserves a region which can be remodelled into a collagen and fibroblast rich dermal replacement. The presence of fibroblasts within the scaffold is essential to support the growth of a stratified and differentiated epithelium, the crosstalk between epidermal keratinocytes and fibroblasts is needed for tissue remodelling.<sup>24, 25</sup> In wound healing, the mid- and late phases are dominated by keratinocyte and fibroblast interactions which drive the formation of granulation tissue.<sup>26</sup> The PHBV layer created here is only 20  $\mu\text{m}$  across, with pores of just over 1  $\mu\text{m}$  has previously been shown to have a porosity 60% porous,<sup>18</sup> and we suggest that this would not prevent cytokine keratinocyte—fibroblast crosstalk which normally occurs across the papillary dermis.

The creation of a functioning epithelium supported by fibroblasts within a dermal matrix is a concept of great interest in the field of regenerative medicine. In the case of large burns where the available skin for autografting is limited, a scaffold capable of being seeded with autologous cells to recreate a functional epithelium would assist surgeons in the management of these patients and reduce the use of allograft material. The majority of bio-engineered skin substitutes are comprised of freeze-dried biopolymer sponges populated with donor dermal fibroblasts alone or in conjunction with keratinocytes.<sup>27, 28</sup> The scaffold presented here is made from fibres known to be

biocompatible and biodegradable over a 1–2 year period<sup>29</sup>, however the rate of degradation can be increased by using PLLA:Polyglycolic acid blends and by sterilisation post production with gamma irradiation. Ideally one wants scaffolds to breakdown without causing any inflammatory problems at a rate to match the rate of remodelling or replacement by the host cells.<sup>30</sup> An electrospun scaffold of biodegradable biocompatible electrospun fibres would be a promising material providing both a functional epithelium and a protected fibroblast rich dermal niche. Such organization is essential to skin development and effective wound healing. The creation of a stratified epithelium is essential, providing a barrier to fluid loss and infection. Thus, to provide the greatest benefits to patients both the dermal and epidermal components need to be viable and well organized.

## 5. CONCLUSIONS

Our study demonstrates the possibilities of making a composite construct with a tri-layered scaffold containing an epidermal layer with an artificial basement membrane and underlying dermal structure. The nano-fibrous PHBV membrane of the tri-layered electrospun scaffold segregating keratinocytes and fibroblasts did not have any negative impact on the attachment and proliferation of keratinocytes and fibroblasts. PHBV nano-fibres were found to promote keratinocyte adhesion and proliferation compared with the mono-layered PLLA surface with keratinocytes and fibroblasts on the upper and lower surface of the scaffold. Further work with this trilayer scaffold will now focus on modifying the dermal region of the scaffold to promote rapid neovascularization when transplanted.

## References and Notes

1. S. MacNeil, *Nature* 445, 874 (2007).
2. M. Varkey, J. Ding, and E. E. Tredget, *Tissue Eng. Part A* 20, 540 (2014).
3. A. el Ghalbzouri, M. F. Jonkman, R. Dijkman, and M. Ponec, *J. Invest Dermatol.* 124, 79 (2005).
4. M. Balasubramani, T. R. Kumar, and M. Babu, *Burns* 27, 534 (2001).
5. D. Breitzkreutz, I. Koxholt, K. Thiemann, and R. Nischt, *Biomed. Res. Int.* 179784 (2013).
6. V. S. LeBleu, B. Macdonald, and R. Kalluri, *Exp. Biol. Med. (Maywood.)* 232, 1121 (2007).
7. D. Breitzkreutz, N. Mirancea, and R. Nischt, *Histochem. Cell Biol.* 132, 1 (2009).
8. F. T. Moutos, L. E. Freed, and F. Guilak, *Nat. Mater.* 6, 162 (2007).
9. M. E. Viney, A. J. Bullock, M. J. Day, and S. MacNeil, *Regen. Med.* 4, 397 (2009).
10. N. Green, Q. Huang, L. Khan, G. Battaglia, B. Corfe, S. MacNeil, and J. P. Bury, *Tissue Eng Part A* 16, 1053 (2010).
11. N. H. Green, Z. Nicholls, P. R. Heath, J. Cooper-Knock, B. M. Corfe, S. MacNeil, and J. P. Bury, *Int. J. Exp. Pathol.* doi: 10.1111/iep.12083 (2014).
12. G. A. El, M. F. Jonkman, R. Dijkman, and M. Ponec, *J. Invest Dermatol.* 124, 79 (2005).
13. K. A. Blackwood, R. McKean, I. Canton, C. O. Freeman, K. L. Franklin, D. Cole, I. Brook, P. Farthing, S. Rimmer, J. W. Haycock, A. J. Ryan, and S. MacNeil, *Biomaterials* 29, 3091 (2008).
14. I. Canton, R. McKean, M. Charnley, K. A. Blackwood, C. Fiorica, A. J. Ryan, and S. MacNeil, *Biotechnol. Bioeng.* 105, 396 (2010).
15. M. Selim, A. J. Bullock, K. A. Blackwood, C. R. Chapple, and S. MacNeil, *BJU. Int.* 107, 296 (2011).
16. N. Nagiah, G. Ramanathan, L. Shobana, S. Singaravelu, U. Sivakumar, S. Tiruchirapalli, T. Natarajan, and S. Tirupattur, *J. Biomater. Tissue Eng.* 3, 624 (2013).
17. L. Di Silvio, N. Gurav, and R. Sambrook, *Med. J. Malaysia, 59 Suppl B* 89 (2004).
18. F. J. Bye, J. Bissoli, L. Black, A. J. Bullock, S. Puwanun, G. C. Reilly, S. MacNeil, K. Moharamzadeh, and A. J. Ryan, *Biomaterials Science* 9, 942 (2013).
19. F. J. Bye, L. Wang, A. J. Bullock, K. A. Blackwood, A. J. Ryan, and S. MacNeil, *J. Vis. Exp.* (2012).
20. C. S. Hughes, L. M. Postovit, and G. A. Lajoie, *Proteomics* 10, 1886 (2010).
21. G. Benton, H. K. Kleinman, J. George, and I. Arnaoutova, *Int. J. Cancer* 128, 1751 (2011).
22. D. Y. Lee and K. H. Cho, *Arch. Dermatol. Res.* 7, 296 (2005).
23. D. R. Ralston, C. Layton, A. J. Dalley, S. G. Boyce, E. Freedlander, and S. MacNeil, *British Journal of Dermatology* 140, 605 (1999).
24. G. Sawicki, Y. Marcoux, K. Sarkhosh, E. E. Tredget, and A. Ghahary, *Mol. Cell Biochem.* 269, 209 (2005).
25. G. C. Ebersole, P. M. Anderson, and H. M. Powell, *J. Biomech.* 43, 3183 (2010).
26. S. Werner, T. Krieg, and H. Smola, *J. Invest Dermatol.* 127, 998 (2007).
27. S. T. Boyce, R. J. Kagan, K. P. Yakuboff, N. A. Meyer, M. T. Rieman, D. G. Greenhalgh, and G. D. Warden, *Ann. Surg.* 235, 269 (2002).
28. G. Erdag and R. L. Sheridan, *Burns* 30, 322 (2004).
29. K. A. Blackwood, R. McKean, I. Canton, C. O. Freeman, K. L. Franklin, D. Cole, I. Brook, P. Farthing, S. Rimmer, J. W. Haycock, A. J. Ryan, and S. MacNeil, *Biomaterials* 29, 3091 (2008).
30. P. Deshpande, R. McKean, K. A. Blackwood, R. A. Senior, A. Ogunbanjo, A. J. Ryan, and S. MacNeil, *Regen. Med.* 5, 395 (2010).

Received: xx xxxx xxxx. Accepted: xx xxxx xxxx.